Frequency dispersion of complex permeability in Mn–Zn and Ni–Zn spinel ferrites and their composite materials

Takanori Tsutaoka[a)]
Department of Science Education, Graduate School of Education, Hiroshima University, 1-1-1, Kagamiyama, Higashi-Hiroshima 739-8524, Japan

(Received 7 October 2002; accepted 5 December 2002)

Complex permeability spectra $\mu^* = \mu' - i\mu''$ for two types of spinel ferrites (Ni–Zn ferrite and Mn–Zn ferrite) and their composite materials have been investigated. The contribution of domain-wall and natural resonance to the permeability spectra was estimated by the numerical fitting of actual measurement data to a simple formula. Frequency dispersion type of each component, relaxation or resonance, can be estimated from one of the fitting parameters, damping factor. In sintered Mn–Zn ferrite, domain-wall contribution is dominant and gyromagnetic spin resonance or relaxation-type magnetization rotation is large in Ni–Zn ferrite. However, relaxation character is dominant in both Mn–Zn and Ni–Zn ferrite composite materials. In composite materials, the permeability value can be scaled by the ferrite particle content using a simple model concerning demagnetizing field. This analysis is useful in designing the permeability spectra of ferrite composite materials. © *2003 American Institute of Physics.* [DOI: 10.1063/1.1542651]

I. INTRODUCTION

For electromagnetic devices such as inductors, converters, or electromagnetic wave absorbers, ferrite materials are useful and complex permeability of ferrites is an important factor. Thus, many investigations have been carried out in experimental and theoretical bases.[1–5] In particular, spinel ferrites such as Ni–Zn ferrite and Mn–Zn ferrite are the typical materials. Ni–Zn ferrites have relatively high permeability up to about 100 MHz and are widely used in rf devices. Though the Mn–Zn ferrite can have larger permeabilities than the Ni–Zn ferrite in the low-frequency region, permeability decreases rapidly with increasing frequency. Thus, high performance of this ferrite is restricted below about several MHz. In the frequency range from rf to microwave, the permeability spectra of ferrite materials can be characterized by the different magnetizing mechanisms; domain-wall motion, magnetization rotation, and gyromagnetic spin rotation.[6–10] In Mn–Zn ferrite, the effect of eddy current loss must be taken in to account in permeability spectra.[11,12] Generally, domain-wall motion and gyromagnetic spin rotation give the resonance-type frequency dispersion but magnetization rotation has a relaxation-type one. In the polycrystalline ferrite, the frequency dispersion of gyromagnetic resonance (natural resonance) can also be the relaxation type due to high damping factor of gyromagnetic spin motion; magnetic spectra are broadened. This is revealed in the study of permeability spectra under external dc magnetic field; permeability spectra of Mn–Zn ferrite has a relaxation-type dispersion in the almost single-domain state under about 1000 Oe.[13] Further, the domain-wall resonance is possible to have both relaxation- and resonance-type dispersions.[14] Therefore, the complex permeability spectrum of domain-wall motion was treated by the superposition of the two types of frequency dispersion (resonance and relaxation) in the low-frequency region.[15] In the view point of the application of ferrite to high-frequency devices, phenomenological treatment of permeability dispersion was also carried out using resonance and relaxation formulas.[16,17]

On the other hand, ferrite composite materials, in which ferrite particles are embedded in a binder matrix, have been the subjects of considerable interest. A number of studies on the permeability of ferrite composite materials have been performed. Theoretical studies on the permeability spectra of composite materials have been carried out using approximation models such as effective medium theory.[18–23] We have studied the complex permeability of a Ni–Zn ferrite and its composite materials in the viewpoint of device material designing, and have shown that the ferrite composite materials can have higher permeability than sintered ferrite in the 100 MHz region.[24,25] In Ni–Zn ferrite composite materials, the frequency dispersion of permeability can be fitted by a formula containing two components, resonance-type domain-wall motion and relaxation-type magnetization rotation[24,30] and permeability value can be evaluated by a simple model, in which we consider the magnetic circuit of ferrite particles and resin layers. This model, which was first introduced for the polycrystalline ferrite containing nonmagnetic grain boundary,[26] is a suitable explanation for the complex permeability in the composite materials. This type of analysis has also been made for Ni–Zn ferrite–epoxy composites.[27] We also have investigated the Mn–Zn ferrite and its composite materials and pointed out that the eddy current can affect the high-frequency permeability.[28] Since sintered Mn–Zn ferrite is a semiconductor and has relatively high conductivity at room temperature, the skin depth effect must be considered for high-frequency dispersion. However, we can ignore the eddy current effect in Mn–Zn ferrite composite materials due to the increase of electrical resistivity in composite structure.[32] On the other hand, permeability spectra of Mn–Zn ferrite can not be explain by the combination of resonance-type domain-wall motion and relaxation-type

a)Electronic mail: tsutaok@hiroshima-u.ac.jp

magnetization rotation. This is owing to the fact that the high-frequency permeability is not a simple relaxation type. Thus, we must consider both the natural resonance and the magnetization rotation in high-frequency permeability spectra. In this study, we have carried out detailed investigations on the permeability spectra of two types of spinel ferrites (a Ni–Zn ferrite and a Mn–Zn ferrite) in the frequency range up to several GHz. The contribution of the domain-wall and natural resonance or magnetization rotation to the permeability spectra has been estimated by the numerical fitting of actual measurement data to the simple formula having six dispersion parameters for sintered ferrite and composite materials. In this treatment, we can estimate the frequency dispersion characteristics (resonance or relaxation) from the value of damping factors. In this sense, this treatment includes both the magnetization rotation and gyromagnetic resonance for high-frequency permeability spectra. Furthermore, permeability variation with ferrite content in both the ferrite composite materials was examined using a simple model considering a magnetic circuit.[24,25]

II. EXPERIMENT

Sintered ferrites used in this study are commercially available Ni–Zn and Mn–Zn ferrite. The composition of these two types of ferrite samples determined by the electron probe microanalysis method is $Ni_{0.24}Zn_{0.65}Fe_{2.04}O_4$ and $Mn_{0.53}Zn_{0.41}Fe_{2.06}O_4$, respectively. Ferrite particles were prepared by mechanical grinding of sintered ferrite cores and particle size was controlled between 45 and 75 μm. Ferrite composite materials were made by the following process: (1) mixing ferrite particles with polyphenylene sulfide (PPS) resin powder, (2) melting the resin at 300 °C, and (3) pressing the mixture at a pressure of 1000 kg/cm^2 in the cooling process down to the room temperature. Ferrite content was estimated using the density values of the sintered ferrite ρ_f, PPS resin ρ_m, and the composite materials ρ, by measuring the specific gravity. In order to measure complex permeability spectra, obtained samples were cut into the troidal form with an inner diameter of 3.03 mm and with an outer diameter of 7.0 mm. Thickness of samples were controlled less than 2 mm for high-frequency measurements to avoid the skin depth effect in sintered Mn–Zn ferrite. Complex permeability of ferrite and ferrite composite materials were measured by a coaxial line technique in the frequency range from 100 kHz to 10 GHz using an impedance analyzer (HP4194A : 100 kHz to 100 MHz) and a network analyzer (HP8753E and HP8720B : 10 MHz to 10 GHz). Complex permeability measurements under external magnetic field were performed using a solenoid-type electromagnet in the magnetic field up to 1000 Oe.[29]

III. PERMEABILITY SPECTRA OF SINTERED FERRIETE AND COMPOSITE MATERIALS

Figure 1 shows the complex relative permeability spectra of a sintered Ni–Zn ferrite and its PPS composite materials [(a) real part μ' and (b) imaginary part μ'']. For sintered ferrite, the real part μ', which is about 1400 in the low-frequency region, begins to decrease at about 1 MHz. The imaginary part μ'' has a maximum of about 800 at around 2

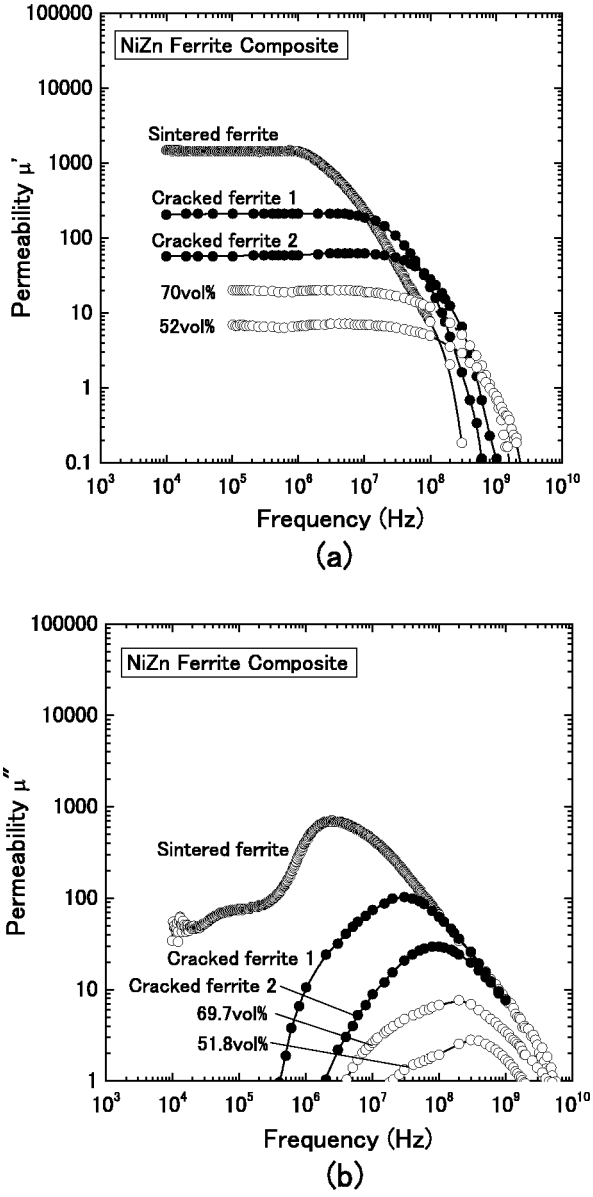

FIG. 1. Complex permeability spectra of Ni–Zn ferrite composite materials.

MHz. Permeability μ' in the high-frequency region from 1 to 100 MHz depends inversely proportional on the frequency. This is a relaxation character. Cracked ferrites were prepared by cracking the sintered core and by bonding them together. In this process, some nonmagnetic gaps are introduced into the sintered body. Thus, the cracked ferrites are considered to be the composite materials with high ferrite content. It can be seen that the frequency dispersion characteristic of cracked ferrites is in the intermediate state between the sintered ferrite and PPS composites. With decreasing ferrite content, the permeability value at low frequency decreases continuously. Simultaneously, the dispersion frequency at which μ' begins to decrease, shifts to a higher frequency region with decreasing ferrite content. As a result, high-frequency permeability is larger in Ni–Zn ferrite composites than that in sintered Ni–Zn ferrite. The resonance frequency shift can also be seen in μ'' spectra; the maximum frequency of μ'' increases with decreasing ferrite content. Since there is a restriction of the ferrite content in particle dispersed composite structure,

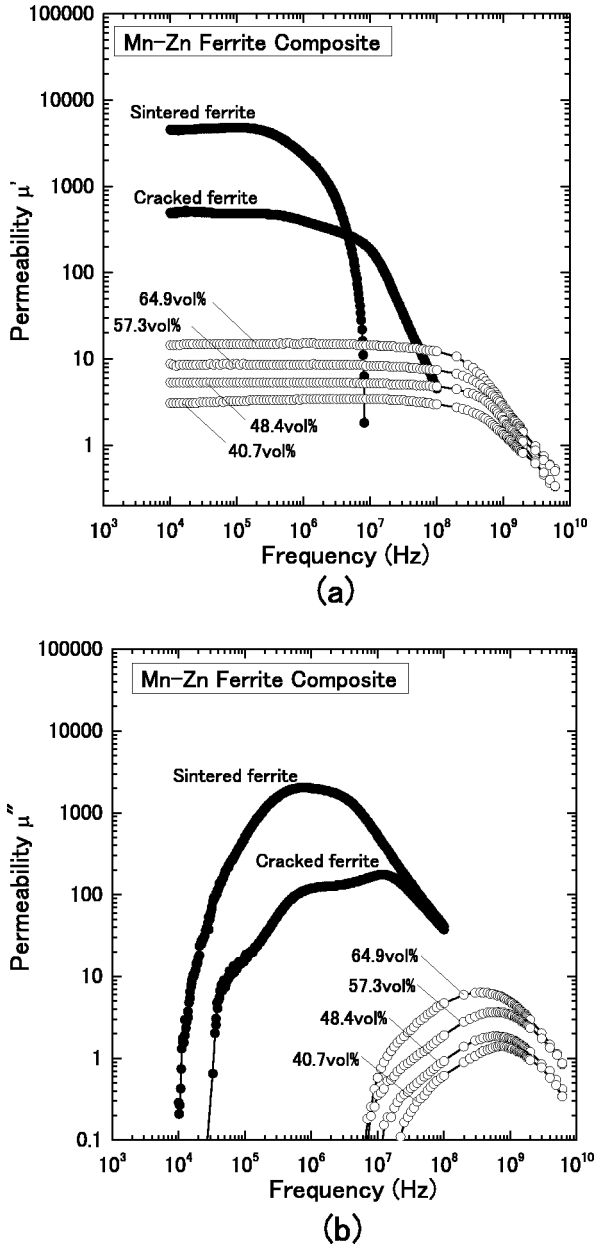

FIG. 2. Complex permeability spectra of Mn–Zn ferrite composite materials.

ferrite particle content cannot be increased beyond a certain value of packing fraction.

In Fig. 2, complex permeability spectra for Mn–Zn ferrite composite materials are presented. In sintered Mn–Zn ferrite, the permeability value at low frequency is about 4000 and dispersion frequency is located around 100 kHz, which is lower than that for Ni–Zn ferrite. In Mn–Zn ferrite, high-frequency permeability μ' above 1 MHz decreases rapidly; this is a resonance character. However, a cracked ferrite and ferrite composite materials have the relaxation-type frequency dispersion. This indicates that though sintered ferrite has a resonance character of permeability; composite materials have the relaxation-type permeability spectra. In the cracked Mn–Zn ferrite, there are two maxima in the μ'' spectrum. It is considered that these correspond to the domain-wall and the natural resonance peaks. In Mn–Zn ferrite composite materials, dispersion frequencies located above 100 MHz and frequency dispersion characteristic are also relaxation type, which is similar to that for Ni–Zn ferrite composite materials.

IV. CONTRIBUTION OF DOMAIN-WALL AND NATURAL RESONANCE TO PERMEABILITY SPECTRA

In polycrystalline ferrite, the frequency dispersion of permeability can be characterized by the superposition of the two types of magnetic resonance (domain-wall and natural resonance) and a relaxation-type magnetization rotation. In the absence of the external magnetic field, a gyromagnetic resonance can be occurred by the internal magnetic field produced by the crystalline magnetic anisotropy. Since natural resonance can also have relaxation-type frequency dispersion due to the high damping of spin motion, it is difficult to separate the contribution of magnetization rotation and gyromagnetic resonance in permeability spectra. Thus, we employ the simple frequency dispersion formula containing two components owing to domain-wall and gyromagnetic spin motion[5]

$$\mu = 1 + \chi_d + \chi_s = 1 + \frac{\omega_d^2 \chi_{d0}}{\omega_d^2 + \omega + i\omega\beta} + \frac{(\omega_s + i\omega\alpha)\omega_s \chi_{s0}}{(\omega_s + i\omega\alpha)^2 - \omega^2}. \tag{1}$$

Here, χ_d and χ_s are magnetic susceptibility for domain-wall and gyromagnetic spin motions, ω_d and ω_s are resonance frequencies of domain-wall and spin components, χ_{d0} and χ_{s0} are the static magnetic susceptibility of each component, α and β are damping factors, and ω is the frequency of external electromagnetic fields. In this formula, if α is large enough to unity ($\alpha \to \infty$), the χ_s can be approximated to the relaxation-type frequency dispersion,

$$\mu = 1 + \frac{\omega_d^2 \chi_{d0}}{\omega_d^2 + \omega + i\omega\beta} + \frac{\chi_{s0}}{1 + i\dfrac{\omega}{\omega_r}}, \tag{2}$$

where ω_r is the relaxation frequency. Therefore, relaxation-type magnetization rotation can be estimated by the high value of damping factor in formula (1).

The real and imaginary parts of the formula (1) can be derived as follows,

$$\mu' = 1 + \frac{\omega_d^2 \chi_{d0}(\omega_d^2 + \omega^2)}{(\omega_d^2 - \omega^2)^2 + \omega^2\beta^2} + \frac{\chi_{s0}\omega_s^2[(\omega_s^2 + \omega^2) + \omega^2\alpha^2]}{[\omega_s^2 - \omega^2(1+\alpha^2)]^2 + 4\omega^2\omega_s^2\alpha^2}, \tag{3}$$

$$\mu'' = \frac{\chi_{d0}\omega\beta\omega_d^2}{(\omega_d^2 - \omega^2)^2 + \omega^2\beta^2} + \frac{\chi_{s0}\omega_s\omega\alpha[\omega_s^2 + \omega^2(1+\alpha^2)]}{[\omega_s^2 - \omega^2(1+\alpha^2)]^2 + 4\omega^2\omega_s^2\alpha^2}. \tag{4}$$

Measured complex permeability data can be fitted to this formula using six fitting parameters ω_d, ω_s, χ_{d0}, χ_{s0}, α, and β. Figure 3 shows the permeability spectra of sintered Mn–Zn [Fig. 3(a)] and Ni–Zn [Fig. 3(b)] ferrites with fitting

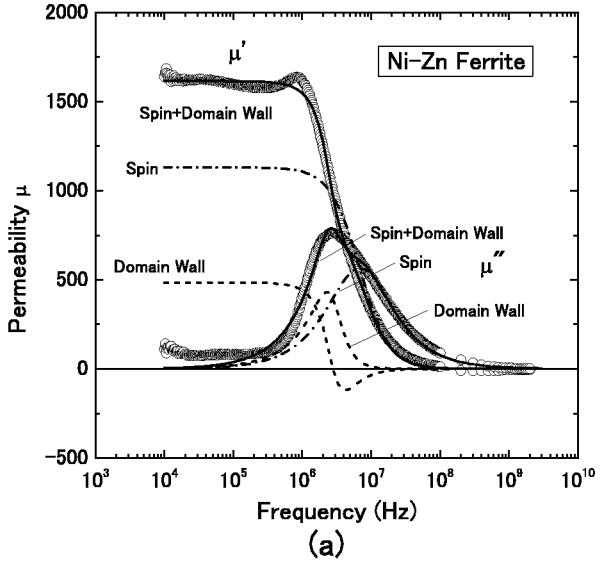

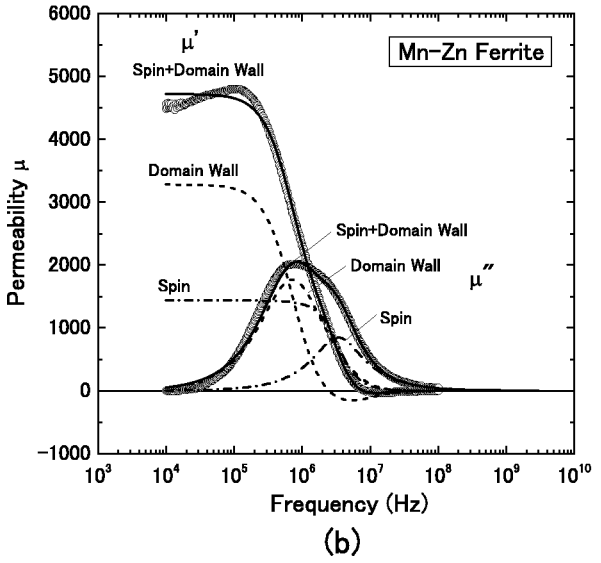

FIG. 3. Complex permeability spectra of a sintered Ni–Zn and Mn–Zn ferrite. Solid, dotted, and dashed–dotted lines are calculation curves for domain-wall and spin components.

curves. In Fig. 3 solid, the dotted, and dashed–dotted lines are the calculation curves obtained for the numerical fitting using a nonlinear least mean square fitting. Obtained dispersion parameters are shown in Table I. In Ni–Zn ferrite, the damping factor of gyromagnetic resonance is large and resonance frequency is over 1000 MHz. This fact indicates that the spin contribution of Ni–Zn ferrite is a relaxation type and this resonance frequency does not have a physical meaning. The maximum frequency of the spin component is located at

TABLE I. Permeability dispersion parameters of sintered Mn-Zn and Ni-Zn ferrite for spin and domain wall resonance.

		Domain Wall Component			Spin Component		
	Density (g/cc)	χ_{d0}	ω_d (MHz)	β	χ_{s0}	ω_s (MHz)	α
Mn-Zn Ferrite	4.90	3282	2.5	9.3×10^6	1438	6.3	1.28
Ni-Zn Ferrite	5.20	485	2.8	3.5×10^6	1130	1100	161

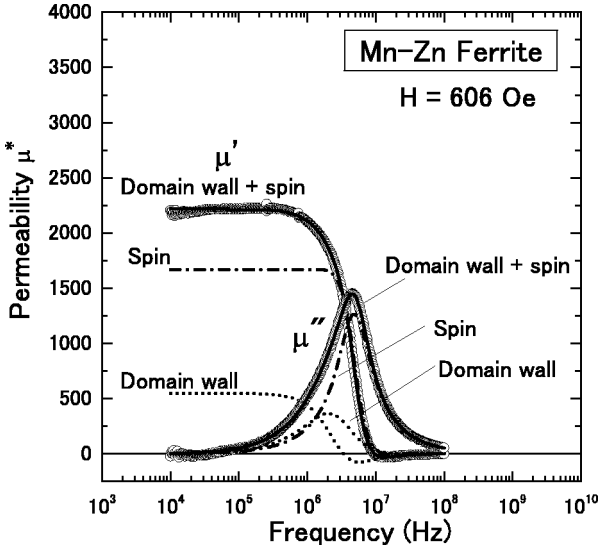

FIG. 4. Complex permeability spectra of a sintered Mn–Zn ferrite under external magnetic field. Solid, dotted, and dashed–dotted lines are calculation curves for domain-wall and spin components.

6.76 MHz and this value is far from the estimated resonance frequency. The maximum frequency of μ'' can be derived by $d\chi''/d\omega=0$. Therefore, we can obtain the following relation between maximum frequencies and damping factors for gyromagnetic resonance,

$$\omega^s_{\chi''\max}=\frac{\omega_s}{\sqrt{\alpha^2+1}}, \tag{5}$$

and for domain-wall resonance,

$$\omega^d_{\chi''\max}=\frac{1}{6}\sqrt{12\omega_d^2-6\beta^2+6\sqrt{16\omega_d^4-4\omega_d^2\beta^2+\beta^4}}. \tag{6}$$

From Eqs. (5) and (6), the maximum frequencies in μ'' spectrum ($\omega_{\mu''\max}$) shift to lower frequency by the increase of damping for spin and domain-wall motion. Since the gyromagnetic resonance can be relaxation type due to the large

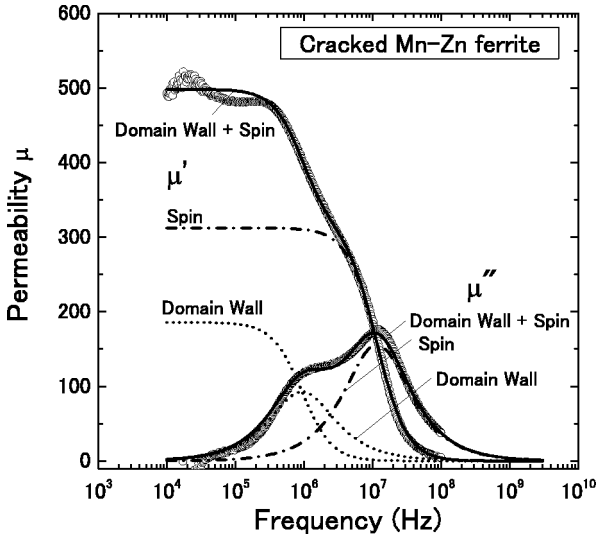

FIG. 5. Complex permeability spectra for cracked sintered Mn–Zn ferrite. Solid, dotted, and dashed–dotted lines are calculation curves for domain-wall and spin components.

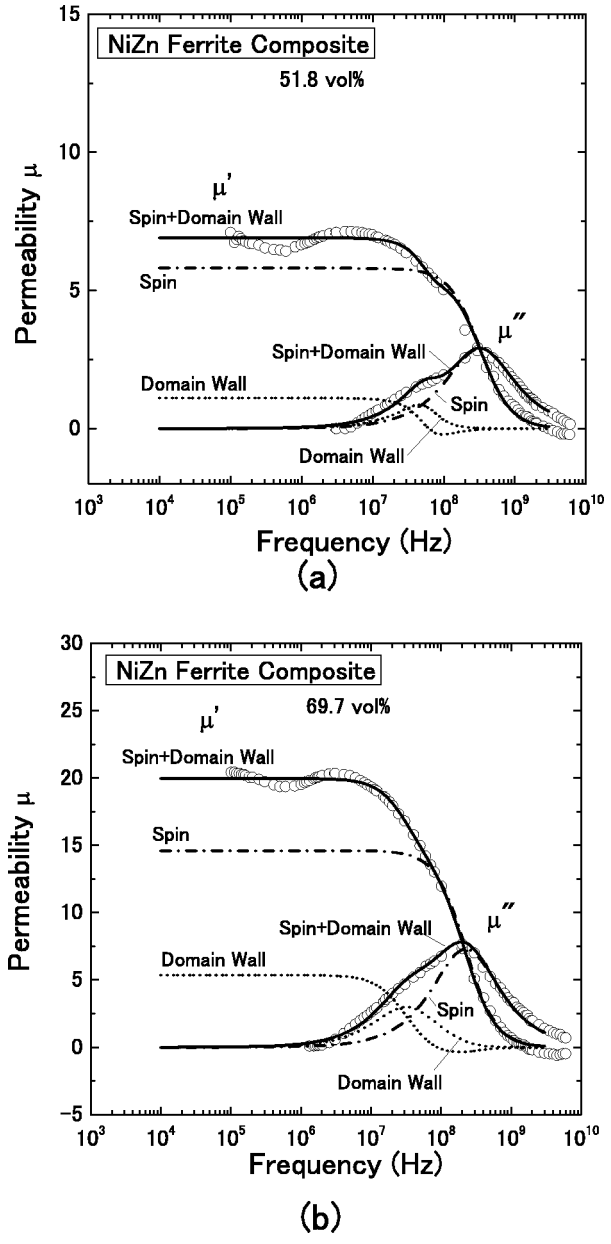

FIG. 6. Complex permeability spectra for Ni–Zn ferrite composite materials. Solid, dotted, and dashed–dotted lines are calculation curves for domain-wall and spin components.

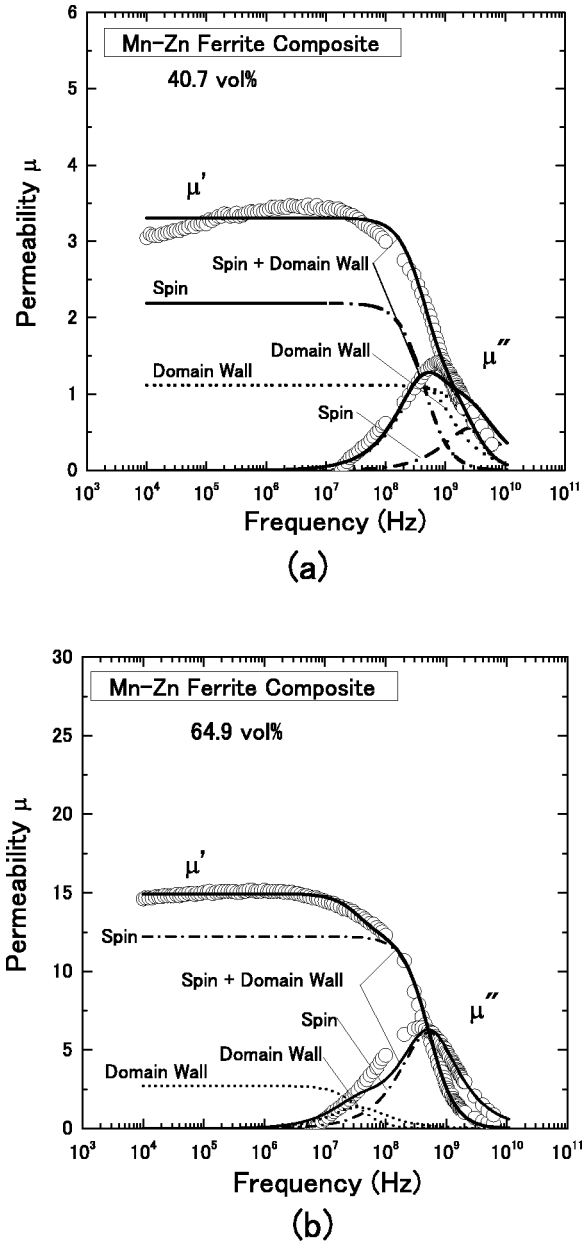

FIG. 7. Complex permeability spectra for Mn–Zn ferrite composite materials. Solid, dotted, and dashed–dotted lines are calculation curves for domain-wall and spin components.

damping of spin motion, especially in Ni–Zn ferrite, the maximum frequency of μ'' is much lower than the resonance frequency and the $\omega_{\mu''\max}$ corresponds to the relaxation frequency ω_r. For Ni–Zn ferrite, the maximum frequency of μ'' for spin component is 7.0 MHz from Eq. (5) using the obtained damping value $\alpha=161$. This is fairly good agreement with the $\omega_{\mu''\max}$ value of 6.76 MHz for the fitting curve in Fig. 3(b). For the domain-wall component, $\omega_{\mu''\max}$ is estimated to be 1.2 MHz from Eq. (6), and fitted value is 708 kHz in Fig. 3(b). It should be noted that the domain-wall condition is sensitive to the inner stress or distribution of grains.

These results indicate that the permeability spectra of spinel ferrites can be described by the two kinds of resonance formula. From fitting data, domain-wall contribution is dominant in the Mn–Zn ferrite and the gyromagnetic one is dominant in the Ni–Zn ferrite. Since spin contribution in Ni–Zn ferrite is relaxation type, we can estimate the high-frequency component as spin rotation.[24,30] These are supported by the magnetic field effect on the permeability spectra. Permeability for both ferrites is strongly suppressed under external magnetic field about 1000 Oe by almost diminishing magnetic domains[31,32] Figure 4 shows the permeability spectra of this Mn–Zn ferrite under a magnetic field of 606 Oe. Estimated dispersion components are $\omega_s=6.47$ MHz, $\omega_d=3.41$, $\chi_{s0}=1665$, $\chi_{d0}=550$, $\alpha=0.87$, $\alpha=6.47\times10^6$, respectively. From this, we can see that the both damping factors decrease and the domain-wall contribution is strongly suppressed under external magnetic field.

On the other hand, since Mn–Zn ferrite has a relatively large electrical conductivity, the effect of eddy current must be considered in the high-frequency region. The skin depth

TABLE II. Permeability dispersion parameters of sintered Ni-Zn and Mn-Zn ferrites and their composite materials.

	Density (g/cc)	Content (vol.%)	δ/D	Domain Wall Component			Spin Component			
				χ_{d0}	ω_d (MHz)	β	χ_{s0}	ω_s (MHz)	ω_r (MHz)	α
Ni-Zn ferrite composite										
Sintered ferrite	5.20	100	0	649	3.5	5.7×10^6	818	1100	7.97	161
NZP70	4.02	69.7	0.13	5.4	31.4	2.7×10^8	14.6	270×10^3	233	1.2×10^3
NZP50	3.32	51.8	0.25	1.1	44.4	1.4×10^8	5.8	13×10^6	329	3.9×10^4
Mn-Zn ferrite composite										
Sintered ferrite	4.90	100	0	3282	2.5	9.3×10^6	1438	6.3	3.39	1.28
MZP60	3.69	64.9	0.16	3.9	296	2.0×10^9	12.2	875	533	2.31
MZP40	2.80	40.7	0.35	2.2	786	2.6×10^9	1.1	55×10^8	2800	2.0×10^4

effect of an electromagnetic wave affects the permeability spectra above several MHz, which is estimated by the measurements of ac resistivity.[31] However, we can measure the intrinsic spin component using a thin specimen whose thickness is less than the skin depth. For this Mn–Zn ferrite, skin depth, which is estimated from the permittivity and resistivity measurements,[32] is about 1 mm at 100 MHz. Therefore, we can avoid the eddy current effect using the sample thickness below about 2 mm for the Mn–Zn ferrite up to several 100 MHz.

V. COMPLEX PERMEABILITY OF SPINEL FERRITE COMPOSITE MATERIALS

In Fig. 5, the complex permeability spectra μ^* for a cracked Mn–Zn ferrite are presented. The cracked ferrite is considered to be a kind of composite material having a nonmagnetic region.[24] Thus, the demagnetizing field affects the frequency dispersion of permeability. There are two peaks corresponding to the domain wall and spin resonance in the μ'' spectrum in Fig. 5. Estimated dispersion components by the numerical fitting are $\omega_s=3757$ MHz, $\omega_d=126$ MHz, $\chi_{s0}=313$, $\chi_{d0}=186$, $\alpha=324$ and $\alpha=1.71\times10^{10}$, respectively. Compared to the sintered ferrite results, the damping factor increases by introducing the nonmagnetic region in the sintered body. In other words, ferrite composite materials have larger damping factors than sintered ferrite.

Figure 6 shows the complex permeability spectra for Ni–Zn ferrite composite materials, [Fig. 6(a)] 51.8 vol %, and [Fig. 6(b)] 69.7 vol %. Calculation curves are also shown by solid, dotted and dashed–dotted Line in Fig. 6. Dispersion frequency is higher in the 51.8 vol % composite than that in the 69.7 vol % one. Spin contribution is dominant in both ferrite content. The same treatment results are shown in Fig. 7 for Mn–Zn ferrite composite materials, [Fig. 7(a)] 40.7 vol % and [Fig. 7(b)] 64.9 vol %. Almost the same dispersion character as Ni–Zn ferrite composite materials are observed. These results indicate that the domain-wall contribution for permeability decreases in composite materials due to the decrease of domain-walls.

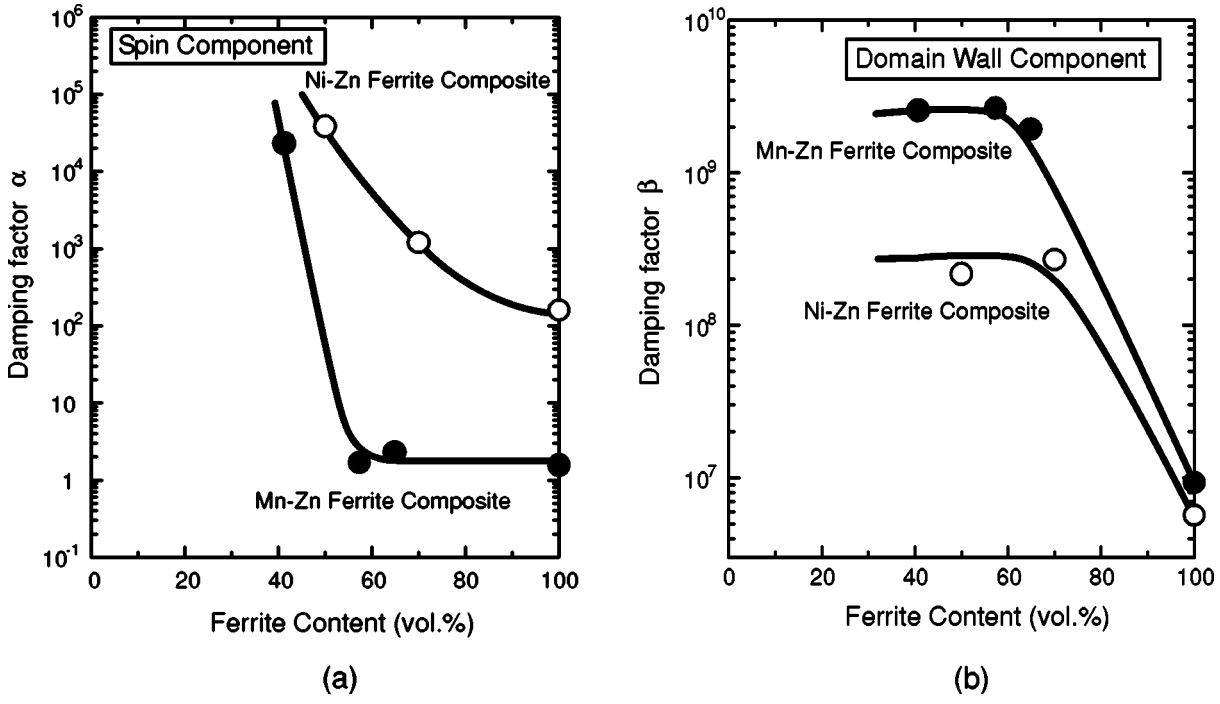

FIG. 8. Damping factors for a Ni–Zn ferrite for a Mn–Zn ferrite as a function of ferrite content.

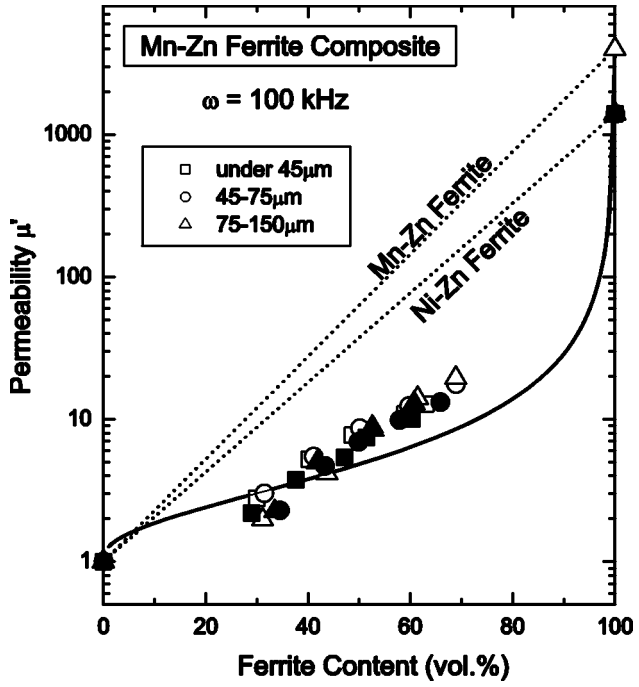

FIG. 9. Absolute permeability at 100 kHz as a function of ferrite content. Dashed lines indicate the logarithmic law. Solid line shows the calculation curve by coherent model.

Dispersion parameters for sintered ferrites and their composite materials are shown in Table II. For Ni–Zn ferrite and its composite materials, obtained resonance frequencies and damping factors are very high. This indicates that the high-frequency permeability is almost completely relaxation type. Therefore, we can apply formula (2) for fitting of Ni–Zn ferrite and its composite materials. Therefore, relaxation frequency ω_r is reasonable to explain the permeability spectra. On the other hand, in Mn–Zn ferrite and its composites, the discrepancy of resonance frequency and relaxation frequency for a spin component is not so large without 40.7 vol % composite. This indicates that resonance-type frequency dispersion exists in the high-frequency permeability spectra in Mn–Zn ferrite and its low ferrite content composites. On the contrary, for the domain-wall component, the damping factor β is large in Mn–Zn ferrite composite materials. Thus, relaxation-type dispersion can be seen in Mn–Zn ferrite composite in domain-wall motion.[15]

Figure 8 shows the damping factors α and β as a function of ferrite content for both Mn–Zn and Ni–Zn ferrite composite materials. In the spin component, Ni–Zn ferrite composite shows high damping even in sintered ferrite and relaxation-type dispersion can be seen. However, in Mn–Zn ferrite composite, resonance character is observed above 60 vol %. In the domain-wall component, though relatively low damping is observed in sintered Mn–Zn and Ni–Zn ferrite, the damping factor increases rapidly when the ferrite content decreases. The damping factor is larger in Mn–Zn ferrite composite than that in a Ni–Zn ferrite composite. This can be attributed to the difference of grain structure between Ni–Zn ferrite and Mn–Zn ferrite; Mn–Zn ferrite contains some impurities in grain boundaries to increase electrical resistivity. Thus the pinning effect of domain-walls can be larger in Mn–Zn ferrite than that in Ni–Zn ferrite. Therefore, the contribution of domain-wall motion to the permeability spectra is considered to be large in Mn–Zn ferrite. The decrease of domain-walls in a ferrite particle dispersed in composite materials brings about the decrease of domain-wall contribution and the loss of resonance character in Mn–Zn ferrite composite materials.

VI. COHERENT MODEL TREATMENTS FOR SPINEL FERRITE COMPOSITE MATERIALS

In Ni–Zn ferrite composite materials, we can apply the coherent model to explain the variation of permeability and

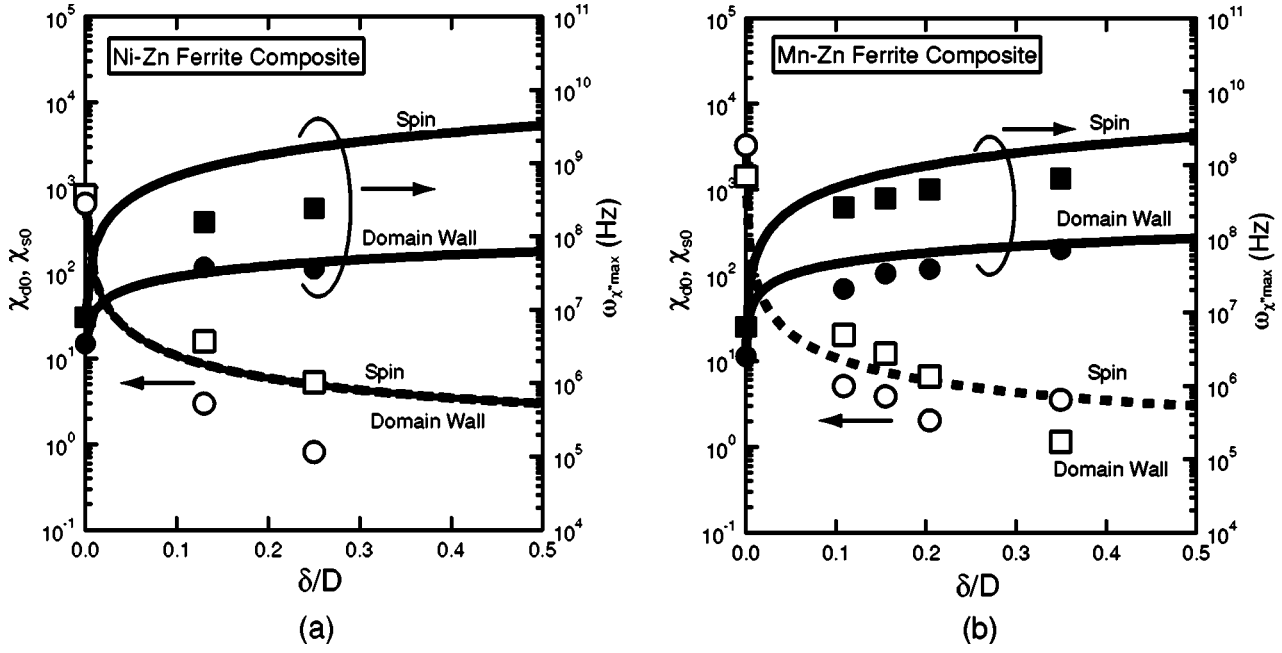

FIG. 10. Variation of permeability dispersion parameters with gap parameter δ/D for Ni–Zn and Mn–Zn ferrite composite materials.

resonance or relaxation frequencies with ferrite particle content.[24,25] In this treatment, permeability of composite materials is given by the following formula considering the magnetic circuit calculation,

$$\mu^*(\omega)=\frac{\mu_B^*\left(1+\frac{\delta}{D}\right)}{1+\mu_B^*\frac{\delta}{D}}. \tag{7}$$

Here, D is the average size of the ferrite particles and $\delta/2$ is the average thickness of the nonmagnetic resin layer. The $\mu_B{}^*$ is the complex permeability of sintered ferrite. Thus, the permeability value of composite materials can be scaled by the gap parameter δ/D. This parameter is connected to the ferrite content in the following manner,

$$\phi=\left(1+\frac{\delta}{D}\right)^{-3}, \tag{8}$$

where, ϕ is the volume ferrite content. Figure 9 shows the absolute permeability value at 100 kHz as a function of ferrite content. The dashed lines in Fig. 9 are the curves by the conventional logarithmic law and solid line is the calculation curve from the coherent model using formulas (7) and (8). Open and solid symbols in Fig. 9 denote the actual measured data in different particle size for both Mn–Zn ferrite and Ni–Zn ferrite composite. The fairly good agreement between the calculation curve and the experimental values is obtained. This result indicates that in composite materials, permeability value is suppressed by the demagnetizing field and almost independent in the type of ferrite and particle size.

Figure 10 shows the variation of permeability dispersion parameters with the gap parameter δ/D for Ni–Zn and Mn–Zn ferrite composite materials. The open symbols in Fig. 10 indicate the dc magnetic susceptibility and solid ones indicate the frequency $\omega_{\chi''\max}$ which is determined by the frequency at which the χ'' has a maximum in calculated permeability spectra using fitted dispersion parameters for spin and domain-wall components. The solid and dashed lines in Fig. 10 indicate the calculation curves by means of this model. The dc magnetic susceptibility decreases and the $\omega_{\chi''\max}$ increases by increasing the gap parameter. Since the gap parameter changes inversely with ferrite content from Eq. (8), these figures indicate that the dc susceptibility increases and the $\omega_{\chi''\max}$ decreases with increasing ferrite content. Therefore, this model can explain qualitatively the variation of the permeability spectra in spinel ferrite composite materials.

VII. CONCLUSIONS

Complex permeability spectra of spinel ferrites (Ni–Zn ferrite and Mn–Zn ferrite) and their composite materials have been studied. The permeability spectra of spinel ferrites can be described by the superposition of the two kinds of resonance formulas (domain-wall resonance and gyromagnetic spin resonance) from the results of the numerical fitting of measured data to the formula. In this treatment, we can evaluate the dispersion character, resonance, or relaxation, from damping factors. In Mn–Zn ferrite composite, spin component has a resonance character in high ferrite content region, but relaxation character is observed in Ni–Zn ferrite composite even in the sintered state. The domain-wall component can also be relaxation type in Mn–Zn ferrite composite. The composite structure brings about the relaxation-type dispersion character in both types of spinel ferrite. A coherent model can be applied to evaluate the permeability value and the frequency dispersion of permeability in both types of spinel ferrite composite materials.

ACKNOWLEDGMENTS

The author is grateful to Dr. K. Hatakeyama and Dr. T. Nakamura of the Himeji Institute of Technology for a fruitful discussion of permeability spectra. The author also expresses his sincere thanks to T. Kasagi and H. Sugitani for sample preparation and characterization. This work was supported by a grant-in aid from the Scientific Research from the Japanese Ministry of Education and Culture.

[1] G. T. Rado, Rev. Mod. Phys. **25**, 81 (1953).
[2] E. F. Schloemann, J. Appl. Phys. **41**, 204 (1970).
[3] A. Globus, J. Phys. **38**, C1-1 (1977).
[4] J. P. Bouchaund and P. G. Zerah, J. Appl. Phys. **67**, 5512 (1990).
[5] *Ferromagnetic Materials* edited by E. P. Wohlfarth (North–Holland, Amsterdam, 1980), vol. 12, p. 243.
[6] G. T. Rado, R. W. Wright, and W. H. Emerson, Phys. Rev. **80**, 273 (1950).
[7] D. Polder and J. Amit, Rev. Mod. Phys. **25**, 89 (1953).
[8] M. Guyot and V. Cagan, J. Magn. Magn. Mater. **27**, 202 (1982).
[9] M. Guyot, T. Merceron, V. Cagan, and A. Messekher, Phys. Status. Solidi **106**, 595 (1988).
[10] J. Jankovskis, V. Yurshevich, and G. Rankis, J. Phys. Colloq. C1-203 (1997).
[11] S. Yamada and E. Otsuki, Proceedings of the Sixth International Conference on Ferrites, 1992, p. 1151.
[12] R. Lebourgeois, P. Perriat, and M. Labeyrie, Proceedings of the Sixth International Conference on Ferrites 1992, p. 1159.
[13] T. Tsutaoka, T. Kasagi, and K. Hatakeyama, J. Eur. Ceram. Soc. **19**, 1531 (1999).
[14] A. Globus and M. Guyot, IEEE Trans. Magn. **6**, 614 (1970).
[15] V. P. Miroshkin, Y. I. Panova, and V. V. Pasynokov, Sov. Phys. Tech. Phys. **23**, 1371 (1978).
[16] Y. Naito, Proceedings of the International Conference on Ferrites 1970, p. 558.
[17] Y. Naito, IEICE Trans. C **J59**, 297 (1976) (in Japanese).
[18] D. Stroud and F. P. Pan, Phys. Rev. B **17**, 1602 (1978).
[19] H. How and C. Vittoria, J. Appl. Phys. **69**, 5138 (1991).
[20] C. A. Grimes and D. M. Grimes, Phys. Rev. B **43**, 10780 (1991).
[21] E. Flavin, F. Boust, and H. Pascard, J. Phys. Colloq. C1-415 (1997).
[22] J. H. Paterson, R. Devine, and A. D. R. Phelps, J. Magn. Magn. Mater. **196**, 319 (1999).
[23] J. L. Mattei, D. Bariou, A. Chevalier, and M. L. Floc'h, J. Appl. Phys. **87**, 4975 (2000).
[24] T. Nakamura, T. Tsutaoka, and K. Hatakeyama, J. Magn. Magn. Mater. **138**, 319 (1994).
[25] T. Tsutaoka, M. Ueshima, T. Tokunaga, T. Nakamura, and K. Hatakeyama, J. Appl. Phys. **78**, 3983 (1995).
[26] M. T. Johnson and E. C. Visser, IEEE Trans. Magn. **26**, 1987 (1990).
[27] K. C. Han, H. D. Choi, T. J. Moon, W. S. Kim, and K. Y. Kim, J. Mater. Sci. **30**, 3567 (1995).
[28] T. Tsutaoka, T. Kasagi, T. Nakamura, and K. Hatakeyama, J. Phys. Colloq. C1-557 (1997).
[29] T. Tsutaoka, T. Nakamura, and K. Hatakeyama, J. Appl. Phys. **82**, 3068 (1997).
[30] T. Nakamura, J. Appl. Phys. **88**, 348 (2000).
[31] T. Tsutaoka, T. Kasagi, and K. Hatakeyama, J. Eur. Ceram. Soc. **19**, 1531 (1999).
[32] T. Tsutaoka, H. Sugitani, T. Kasagi, and K. Hatakeyama, J. Magn. Soc. Jpn. **25**, 943 (2001) (in Japanese).